Yun, X., Brooks, S., Cheng, Y., Hales, A., Lucas, E., McBryde, D., & Quarini, J. (2015). Ice formation in the subcooled brine environment. *International Journal of Heat and Mass Transfer*, *95*, 198 - 205. https://doi.org/10.1016/j.ijheatmasstransfer.2015.12.003

Ice formation in the subcooled brine environment

Abstract

Generating ice in a fluid immiscible with water is relatively easy but considerably more difficult if the chosen fluid is hydrophilic. Our experimental work showed that, ice can be produced when water is introduced to a bath of subcooled brine and it was believed that, the rate of heat transfer between the two fluids needs to be higher than that of mass transfer to allow the formation of ice to occur as a result. Flow rheology, hence the size of the active surface area of the injected water stream, brine temperature and concentration are the key factors influencing how much ice can be made in the process. Conversion ratios of two ice collection methods are compared over a range of brine temperatures and concentrations. The washing method (wet collection) was found to collect up to 27% more ice than dry collection. Washing is also very effective in rinsing off the brine and salt on the ice's surface and the bulk salinity would drop from 13% to 1%. Since the evaporator temperature has to be higher than the eutectic point of brine, it was suggested that, the coefficient of performance, COP, will be very promising. In addition, this way of ice production should achieve higher efficiency than a scraped surface ice maker and it is simpler in that it requires no complex mechanical harvesting equipment, and with the vast liquid-liquid surface areas possible, promises to be able to produce high quantities of ice per unit volume of equipment.

1 Introduction

Ice slurries have a wide range of engineering applications. Due to the latent heat of fusion of ice which results in their high energy storage capacity, ice slurries are used as secondary refrigerant for thermal storage systems [1–3]. Another successful application of ice slurries is the ice pigging technology [4] which is now commercially used in water and food industries. Researches to employ this technology in hydrocarbon industry are also being conducted [5].

It is inherently difficult to achieve a high rate of ice production in industrial environments with simple, easy to maintain equipments whilst pursuing high coefficient of performances, COP. Amongst the existing ice slurry generation mechanisms [2,6–14], scraped surface is the most widely utilised. With a type of freezing point depressant (FPD) added in water, ice would nucleate and propagate on a cold metal surface before it can further develop into a mushy layer. As the mushy layer thickens on the subcooled surface, it acts as an insulator which reduces the rate of heat transfer and ice formation. For this reason, it is then required

to shear off the ice by a mechanical scraper or, less popular, an energy inefficient thermal cycling system to keep the ice layer thin. The mushy layer removal systems require high maintenance cost and increase the size of the equipments. The undesirable growth of ice on cold evaporator surfaces is also a problem for both industrial and domestic freezers and deicing has to be performed on a regular basis [15, 16].

A cheaper and more efficient way of generating ice slurries has two separate stages. In the first stage, water is frozen on a cold surface which is cyclically heated to remove the ice once it has reached a certain thickness [17]. Comminution of this bulk ice with brine supplement then completes the process [18]. Per kilogram of ice slurry, this method can reduce energy usage by 32% compared to a scraped surface ice maker provided that the evaporator temperature is elevated by 20℃, from -30℃ to -10℃ and energy consumption of any auxiliary systems are disregarded [19]. With the ice storage and delivery taken into consideration, 20% of saving maybe achievable in practice [20]. As for the implementation on ice pigging, the pig is produced at the point of delivery where bulk ice is crushed into the correct size, instead of being generated overnight and stored and maintained in a stirrer tank where more power is consumed. Although this way of ice slurry generation is more efficient, it is easy to have the crushed ice to stick together and become larger pieces if the added brine does not fill up the gap between ice particles soon enough and consequently makes it difficult to carry out the 'cafetière test' [21, 22] to detect the ice fraction. Whether the quality of the ice slurries would affect electromagnetic wave attenuation which can be used as the fundamental principle of an online ice fraction detection method [23] is not well understood yet. Another method considered inexpensive is to produce ice slurries or flake ice by means of direct contact which requires neither subcooled surfaces nor mechanisms to maintain the rate of production [10–14]. However, this way of ice production requires the mixing of water, refrigerant and compressor oil, making it suitable for the thermal storage application but cannot be implemented in the food industry.

In this study, a novel method of ice production is proposed whereby ice is generated in a fluid with a temperature below the freezing point of water. Water at about 0℃ is introduced into a bath of brine with a range of salt concentrations by weight (from eutectic point, 23.3% to 21%), at temperatures of about -18℃. Provided the rate of transient heat transfer exceeds that of mass transfer so that the latent heat of fusion can diffuse away quickly, ice would form. Experimental progress is presented in this paper.

Nomenclature

α	thermal diffusivity
ΔG_v	Gibbs energy per unit volume
ΔT	bath supercooling temperature

ΔT_{SLSH}	unuseful superheat in the suction line
η_{isen}	isentropic efficiency
η_{vol}	volumetric efficiency
ν	growth rate of ice
$\phi_v^\dagger$	cafetière ice fraction
σ	Surface energy
A	area
a	constant
C_B	wt% salt in brine
C_w	wt% salt in water
D	mass diffusivity
Gr	Grashof number
Gr_m	mass transfer Grashof number
h_h	heat transfer coefficient
h_m	mass transfer coefficient
m	mass transfer
Nu	Nusselt number
Pr	Prandtl number
Q	available cooling by the refrigeration cycle
q	heat transfer
r^*	Critical radius for nucleation
Ra	Rayleigh number
Ra_m	mass transfer Rayleigh number
Re	Reynolds number
Sc	Schmidt number
Sh	Sherwood number

T_B	brine temperature
T_C	compressor temperature
T_E	evaporator temperature
T_w	water temperature
W^*	Critical energy for nucleation
W_c	compressor work
COP	coefficient of performance

2 Background

2.1 Preliminary experimental observations

It is relatively easy to generate ice when the heat sink fluid is immiscible with water, as in the direct contact method, but considerably more demanding if brine is used instead because water can easily mix with the cooling media in this later case. There are two real life examples that enlightened us to consider making ice with a choice of hydrophilic solution and both of them are based on the fact that heat transfer can be higher than mass transfer in fluids.

The first is the simple water droplet experiment, which is performed by releasing a few drops of water to the surface of a bath of cold brine. If the brine temperature is much lower than 0℃, a disc of ice would form. This phenomenon indicates that the transient heat transfer, mainly by conduction, is higher than mass transfer and the Lewis Number, $Le = Sc/Pr = \alpha/D$, which measures the relative boundary layer thickness of temperature and concentration, in this case should be greater than unity.

Another high Le number example is found in a bottle of naturally stratified brine at a concentration below its saturation. Despite it is well mixed in the first place, a concentration gradient will slowly develop along the bottle and eventually remain unchanged if it is left untouched long enough in a room where the ambient temperature fluctuates from day to nigh; at some point, mass transfer will almost stop while heat transfer continues.

These two observations shows that it is possible to produce ice through introducing water to a bath of subcooled brine provided that the heat and mass transfer is carefully controlled so that the latent heat of fusion can dissipate away from the boundary layer before phase transformation completes.

2.2 Heat and mass transfer fundamentals

Water has low value of thermal conductivity (∼0.5 W/mK) and convection of mass, which consists of advection and diffusion, makes it a good heat transfer media. The driving force of advection is the temperature and concentration led density difference that initiates buoyancy with the presence of gravity. Heat and mass transfer can be expressed in Equation 1a and 1b where h_h and h_m are heat and mas transfer coefficient governed by a range of physical properties.

$$q = Ah_h(T_w - T_B) \tag{1a}$$
$$m = Ah_m(C_w - C_B) \tag{1b}$$

h_h can be determined through the Nusselt number, Nu. In most cases, Nu is a function of the Rayleigh number, Ra, and the Prandtl number, Pr, for natural convection only ($Gr/Re^2 \gg 1$); if not, Nu is a function of Ra alone (2a). In forced convection scenario ($Gr/Re^2 \ll 1$), Nu is a function of the Reynolds number, Re, and Pr (2b). If neither convective regime dominates ($Gr/Re^2 \approx 1$), Nu is a function of Re, Gr and Pr; natural and forced convections are in the same order of magnitude (2c) [24–27].

In natural convection, the boundary layer flow would remain laminar if the distance it has travelled is short enough so that the Grashof number, Gr, is below the order of 9 for a wide range of fluids with various Pr values. One can also use $Ra \sim 10^9$, by recalling that $Ra = GrPr$, as the critical value that marks the transition of a natural convective stream. [28]

$$Nu = f(Ra, (Pr)) \tag{2a}$$
$$Nu = f(Re, Pr) \tag{2b}$$
$$Nu = f(Re, Gr, Pr) \tag{2c}$$

In the heat and mass transfer analogy, the counterpart of Nu is the Sherwood number, Sh, which gives h_m, and the Schmidt number, Sh, substitutes Pr. By replacing the temperature terms with concentration, the corresponding mass transfer Rayleigh number, Ra_m, and mass transfer Grashof number, Gr_m, are used in mass transfer problems. As in the heat transfer analysis, the Re is only considered in the mixed convection scenario (3c) or will dominate the mass transfer in forced convection (3b).

$$Sh = f(Ra_m, (Sc)) \tag{3a}$$
$$Sh = f(Re, Sc) \tag{3b}$$
$$Sh = f(Re, Gr_m, Sc) \tag{3c}$$

2.3 Crystallisation: nucleation and growth

Ice I_h-like hydrogen-bonded clusters are the only molecular groups that can occasionally grow by statistical fluctuations into a stable size and become nucleation sites [29]. The minimum energy required for the existing clusters to develop into a size that do not dissolve back to the bulk fluid is

$$W^* = \frac{16\pi\sigma^3}{3\left(\Delta G_v\right)^2} \tag{4}$$

and the corresponding critical radius is

$$r^* = \frac{2\sigma}{\Delta G_v} \tag{5}$$

Once these nucleation sites have bypassed their critical radii, the subsequent rate of dendritic propagation of ice will be very fast and can be expressed in the form of $\nu = a(\Delta T)^n$ [30–32]. In rapid solidification, the growth of solids can be further subdivided into three configurations: needle invasion, consolidation and plateau [33]. The rapid solidification always has an S-shaped history and is in accord with constructal law [34].

3 Apparatus and procedure

3.1 Experimental apparatus

There are two sets of cooling equipments used to carry out the study. The first is the modified Gelato Chef 2200 ice cream maker with a 1.5 litre aluminium container. It is employed to observe effects of water injection position, flow rheology and brine temperature on ice formation. A digital thermometer detects the temperature of the brine in the container throughout the experiments. The thermometer is made of a K-type thermocouple. The experiment recorded in Video 1 used these equipments.

The experimental apparatus setup illustrated in Figure 1 is later utilised to quantify how much ice can be produced for a given mass of water introduced. The tank is filled up by roughly 30 litres of brine at a range of concentrations. The temperature of the fluid is maintained by a refrigeration unit which uses R134a and its evaporator, at about -30℃, is submerged in the liquid. To control the brine temperature, an aquarium heater is installed at the base of the tank and it is switched on by a control unit if the brine temperature, measured by a K-type thermocouple, falls below the preset value. In addition, a small aquarium pump (200 litre/hour) is placed in the tank to assist the heat transfer between the cold evaporator and the bulk fluid by generating a flow to eliminate the growth of hydrohalite and ice on the evaporator's surface. This pump is only switched on between experiments and is off before the experiment starts so that the fluid is quiescent; there is no bulk fluid motion in the brine phase. The experiment recorded in Video 2 used this setup.

Water is delivered and injected to the cold brine by a glass syringe (100 ml capacity) with 2mm diameter silicone tube attached to its end. The syringe is placed on a table whose height can be adjusted, so to alter the siphon hydrostatic pressure between the inlet (exit of syringe) and outlet of the tube. The flow rate of the water stream can therefore be controlled in this way. Both Video 1 and 2 adopt these equipments when delivering water to the bulk brine. The apparatus used to measure the density of the melted ice solution is the Anton Paar DMA 4500 M. Ice slurries are produced from the ZIEGRA ice machine Model SI 1000 and the brine salinity by weight is set at 5%.

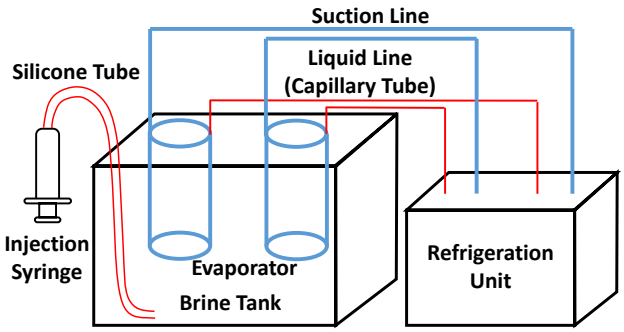

Figure 1: Schematic diagram of experimental apparatus

3.2 Experimental procedure

With the Gelato Chef 2200 setup (Video 1), brine at eutectic concentration is prepared and kept at about -20℃ in a freezer and then poured into the 1.5 litre container where the temperature of the fluid is tracked by the K-type thermometer. The cooling unit is then switched on. The cold evaporator surfaces are in contact with the walls of the container to keep the brine cold. The water to be introduced to the brine is cooled in the same freezer to 2℃ and then sucked into the glass syringe. The differences between releasing water droplets above brine surface and injecting it through the bulk fluid, from the syringe, is compared at first (Section 4.1). To ensure the water temperature at the outlet of the tube are the same for both cases, a fixed length of tube is submerged in the brine and the flow rates are kept identical by adjusting the position of the syringe through the height of the table. Flow rheology can be managed through adjusting the outlet angles as illustrated in Figure 2. The outlet angle can be managed between 90° (Figure 2a) and 0° (Figure 2b) to the horizontal axis. The water stream in the second case, Figure 2b, only has the horizontal velocity component which would result the flow having the highest active surface area with the subcooled liquid (Video 1 and 2). The variation of flow rheology is achieved by adjusting the outlet angle. The change of the rheology of the flow alters surface area over volume ratio of the water stream and it is discussed in Section 4.2. In the last set of experiments with this lower cooling capacity refrigeration system, qualitative effects of brine temperature on the formation of ice is observed. The observations are included in the first paragraph of Section

4.3 of this paper.

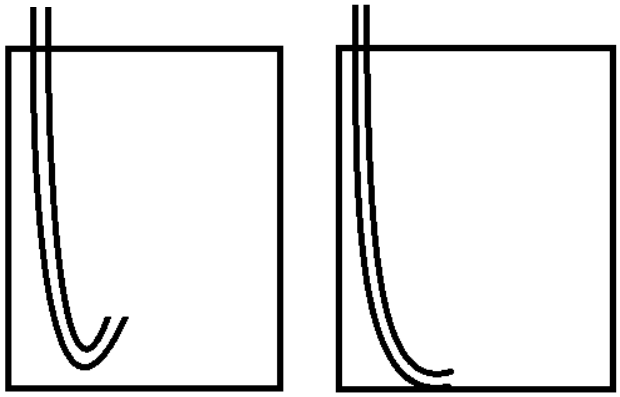

(a) (b)

Figure 2: Flow rheology control

To quantify how much water is converted into ice, 100 ml of water, at 2℃ as in before, is introduce in each experiment across a range of brine temperatures. After each injection, the ice is collected by a finely meshed sieve and weighted on an electronic scale. The sieve is shown in Figure 13b and 13c. There are two ice collection regimes used. In the first, ice is scooped out by the sieve and shook only, whereas it is washed, by 0℃ water, as soon as it is taken out of the tank in the other. The comparison of the two collection regimes can be found in the second paragraph of Section 4.3. Collected ice's density is measured by the density metre once the collected ice is fully melt; the salt concentration by weight in the ice is then derived from this value with reference to Lide [35]. To validate the experimental results from this handbook, we have done some tests and these values match with what were recorded in our lab. The handbook also provides the correlation between brine density and salt concentration by weight. By subtracting the salt mass from the measured value, the net mass of ice collected is obtained; water to ice conversion ratio is hence derived from the net weight of ice.

4 Experimental results and discussion

4.1 Water injection position

The comparison between releasing water droplets above brine surface and injecting it through the bulk fluid, at -16℃ , is shown in Figure 3. When water is introduced to the brine surface (Figure 3a), due to its lower density, it will stay on the top of the subcooled environment and nucleate quickly. The subsequent crystal growth is fast and then slows down. The reason that leads to the reduction in growth rate is because both water and ice are lighter than the brine and they will float on the top of the brine surface and conduction is therefore the form of heat transfer. Since water is poor conductor, the latent heat of fusion of ice will quickly

heat up the surrounding fluid right adjacent to the freezing frontier and cannot be transport to the bulk fluid through mass transfer in form of advection. The rise in local temperature hence slows down the rate of phase transformation.

If water is injected through the brine (Figure 3b), the introduced water will nucleate and propagate on its way to the brine surface and form a rod of ice if the tube exit is kept upright (at 90° to the horizontal axis) as illustrated in Figure 2a. The bulk motion of the stream has enhanced both heat and mass transfer. Advection makes ice to grow faster whereas encourages water to mix with the brine at the same time. The escaping of the unfrozen water away from the freezing frontier can be clearly seen in Video 2.

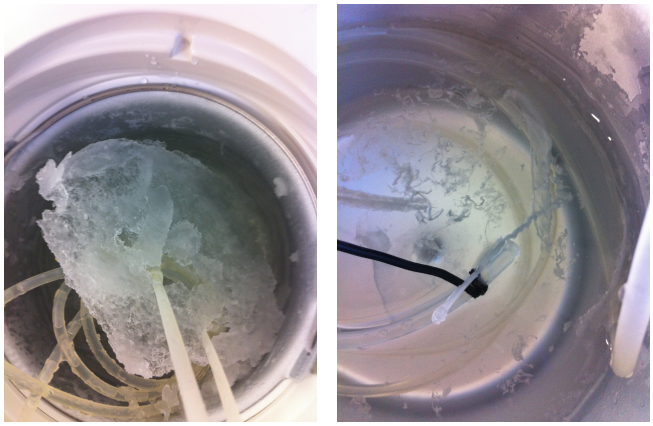

(a) Above brine surface (b) From inside brine

Figure 3: Water injection position comparison

4.2 Flow rheology and area over volume ratio

It was observed that reducing the flow rate does not encourage more ice to be formed but tube blockage. This is because more sensible heat has been extracted when water is still in the tube and it can easily be supercooled and become ice once nucleation is triggered.

Flow rheology, managed by altering vertical and horizontal velocity component of the flow (Figure 2), however has a significant impact on ice formation. Figure 4 and Video 1 showed that, a 'sheet' of ice was produced if the injected water stream only had the horizontal velocity component (Figure 2b). The 'sheet' of ice is always reproducible. If, however, the outlet is kept upright (Figure 2a), a rod of ice may not always appear although the flow rate is kept identical. Pure mixing often happens when water is injected by this way.

The major difference, except the initial vertical velocity, between the two types of injections is the active surface area and hence the area over volume ratio of the stream. Area of contact is a key factor that affects both the rate of heat and mass transfer. According to

the Chilton-Colburn analogy, the change in heat and mass transfer should essentially be the same, however, our experiments have shown otherwise because more ice is generated phase transformation is much more stable when the active surface area is increased. Ice formation certainly has direct correlation to the active surface area and area over volume ratio of the stream. The experiments carried out in Section 4.3 and 4.5 use 0° injection angle.

Figure 4: Flow rheology control

4.3 Effects of brine temperature

It was found that, brine temperature has a strong impact on water to ice conversion ratio. Figure 5 and 6 illustrated the variation in collected mass and mass of ice produced for dry and wet ice collections. Experimental results become unstable when the bath temperature is -17℃ or higher and only the temperature range presented in these figures is studied. If the brine temperature is elevated up to about -13℃, ice can hardly produced by means of injection through the brine. Brine temperature also affects heat and mass transfer between ice and the liquid after ice is generated. At higher bath temperature, ice tends to melt faster.

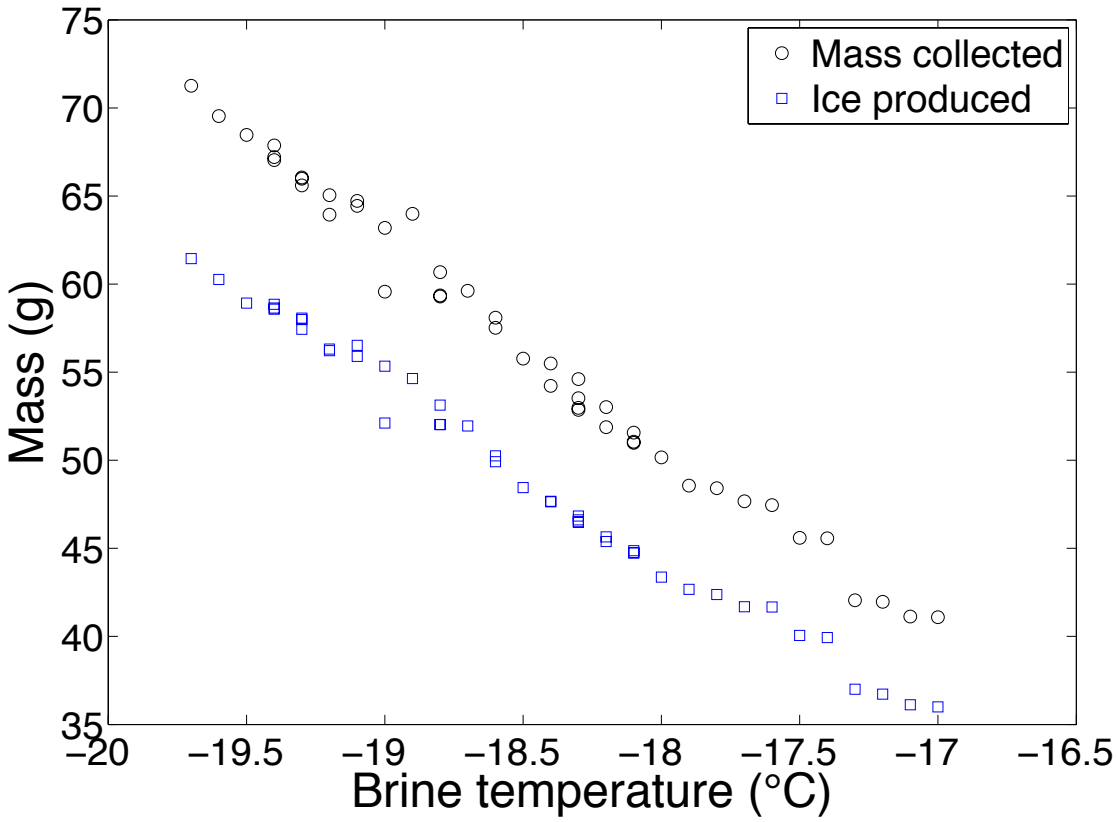

Figure 5: Dry collection at eutectic brine concentration (23.3%wt)

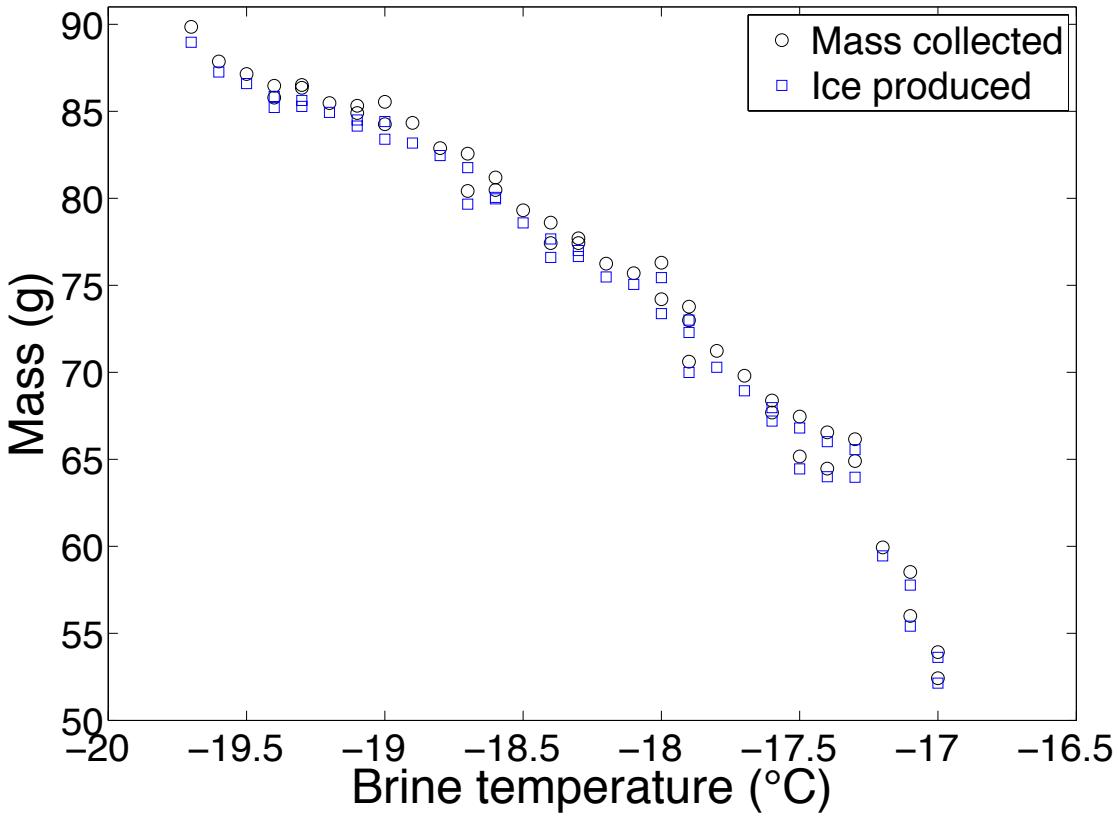

Figure 6: Wet collection at eutectic brine concentration (23.3%wt)

Figure 7 compares the conversion ratios of two ice collection methods. More ice is collected with wet collection regime and the difference in conversion ratio between the two methods is 16 - 27%: at lower brine temperatures, this difference is greater and lowers as the brine temperature elevates. There are two possible reasons causing the conversion ratios of the wet collection much higher than the dry. Firstly, ice has the same temperature as the bulk fluid at the very moment they are taken out of the tank. The washing water will therefore freeze onto the existing ice due to the negative thermal inertia. Since the ice is not dried up before water is poured onto it, the brine in the sieve becomes another source of cold sink and absorbs more latent heat of fusion. Secondly, the collected ice is less rigid at 0℃ and would collapse onto each other and entrap the fluid between the gaps of the ice chips.

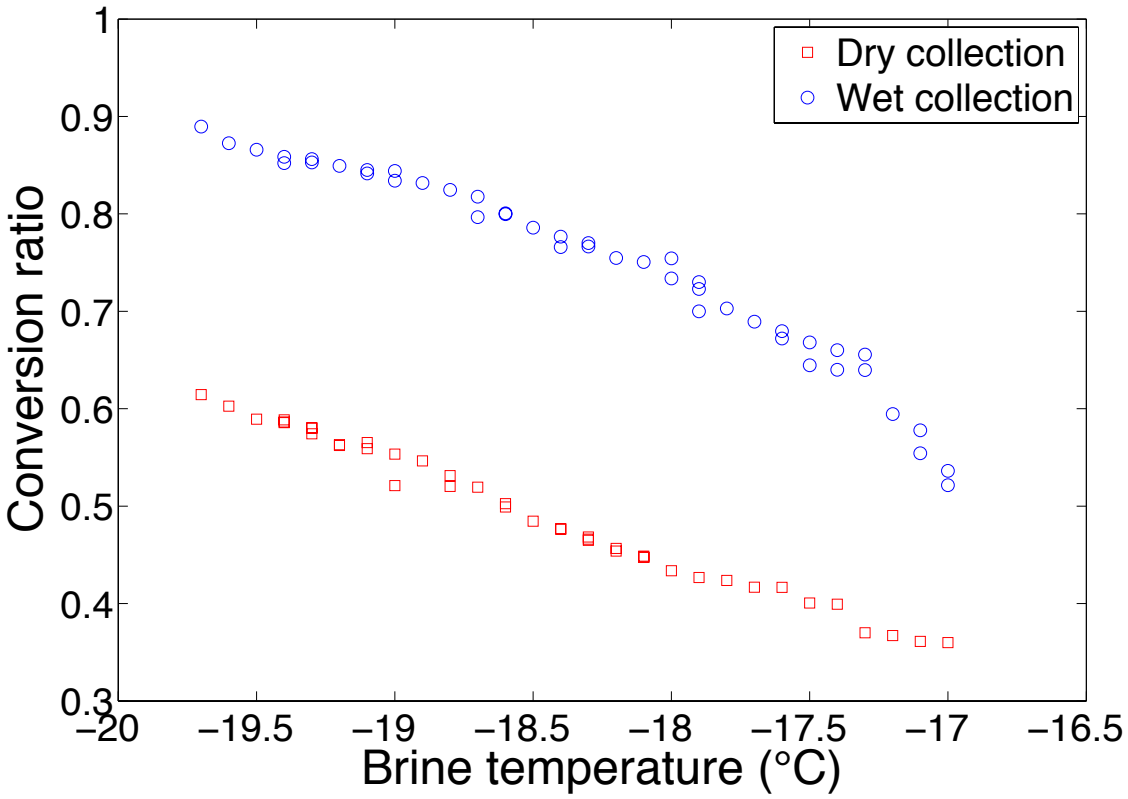

Figure 7: Conversion ratio vs. brine temperature at eutectic brine concentration (23.3%wt)

4.4 Salt entrapment

On average, bulk salinity of the dry collected ice is at about 13% and 1% for the washed ice (Figure 8). The action of washing the ice is very effective in rinsing off the brine and salt that stays on the ice surface. The high salt concentration of the ice in dry collection is quite likely due to the large active surface area, which encourages brine and salt to cling onto the ice. The surface of the generated ice also has rough texture because of the dendritic growth that occurs on the boundary layer where the fluid has a certain degree of mixing. The irregular morphology of these dendrites can trap more rejected salt and high salinity brine onto the ice surface, which effectively elevates the bulk salt concentration of the collected material. The low bulk salinity of the wet collection regime also indicates that, the amount of salt entrapped within the thin ice's structure is negligible. In addition, the salinity of the cold bath, which is between 21% and eutectic point, has no effects on the amount of salt collected with the ice sample at this level of salt concentration.

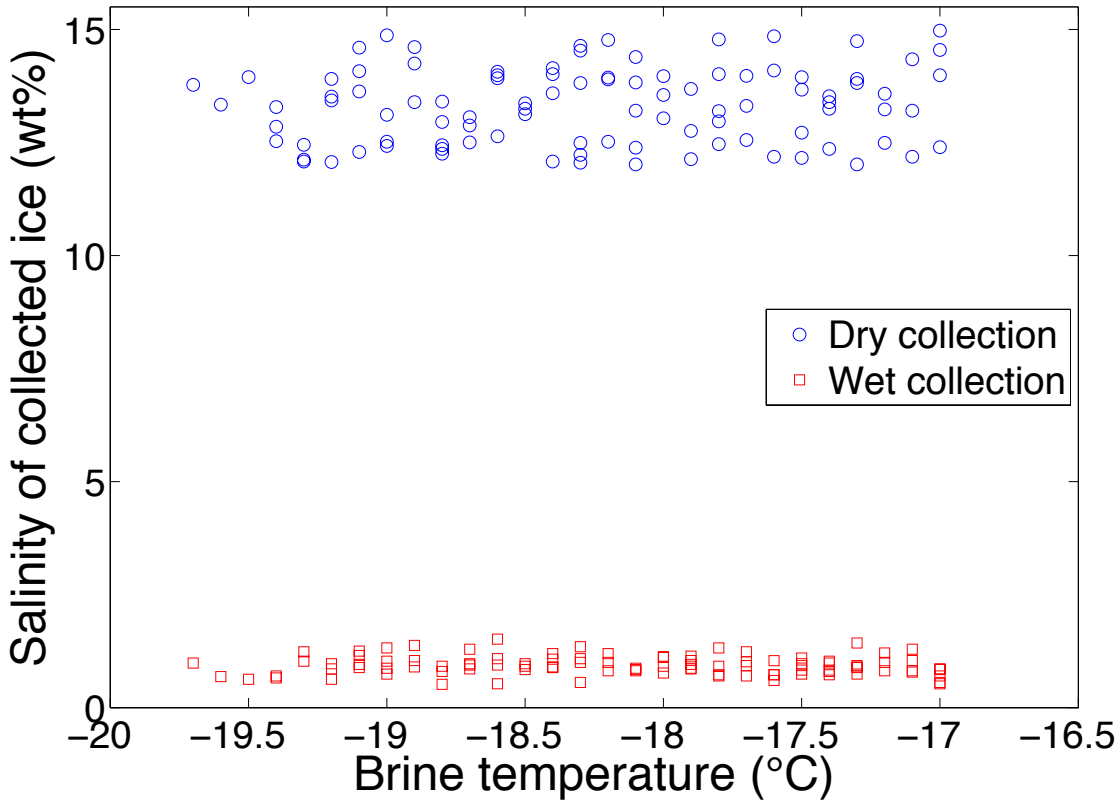

Figure 8: Ice sample salinity vs. brine temperature

The ice particles of ice slurries have low area over volume ratio and this ratio must be lower than the very thin ice 'sheets' produced by our method. To compare the difference in salt content after washing the two types of ice, ice slurries with bulk salinity of 5% is washed with 0℃ water and well shook. It was found that, salt concentrations of the washed ice slurries have strong correlation to the cafetière ice fraction and therefore, the salt concentration of the brine phase and the temperature of the suspension (Figure 9 - 11). However, it is not very clear if the area over volume ratio of the ice affects the salt content after washing is performed from these figures. The percentage error of the cafetière test is 3% [22] and the uncertainty of each salt concentration of the brine phase and the ice slurry temperature are calculated from the corresponding values of $\phi_v^\dagger$.

At higher ice fraction, where the temperature of the ice slurry is lower, the 0℃ washing water tends to freeze and form a thin crust, which barricades the upcoming liquid from rinsing the ice further. The chance of the generation of such shield is very sensitive with ice fraction and the water has more chances to travel through the gaps between the ice particles and lowers the salt concentration as the ice fraction drops. The 60 - 70% ice fraction range looks like the transitional value whence the salinity of the washed ice falls down to a low

level similar to that in the wet collection scenario in Section 4.3.

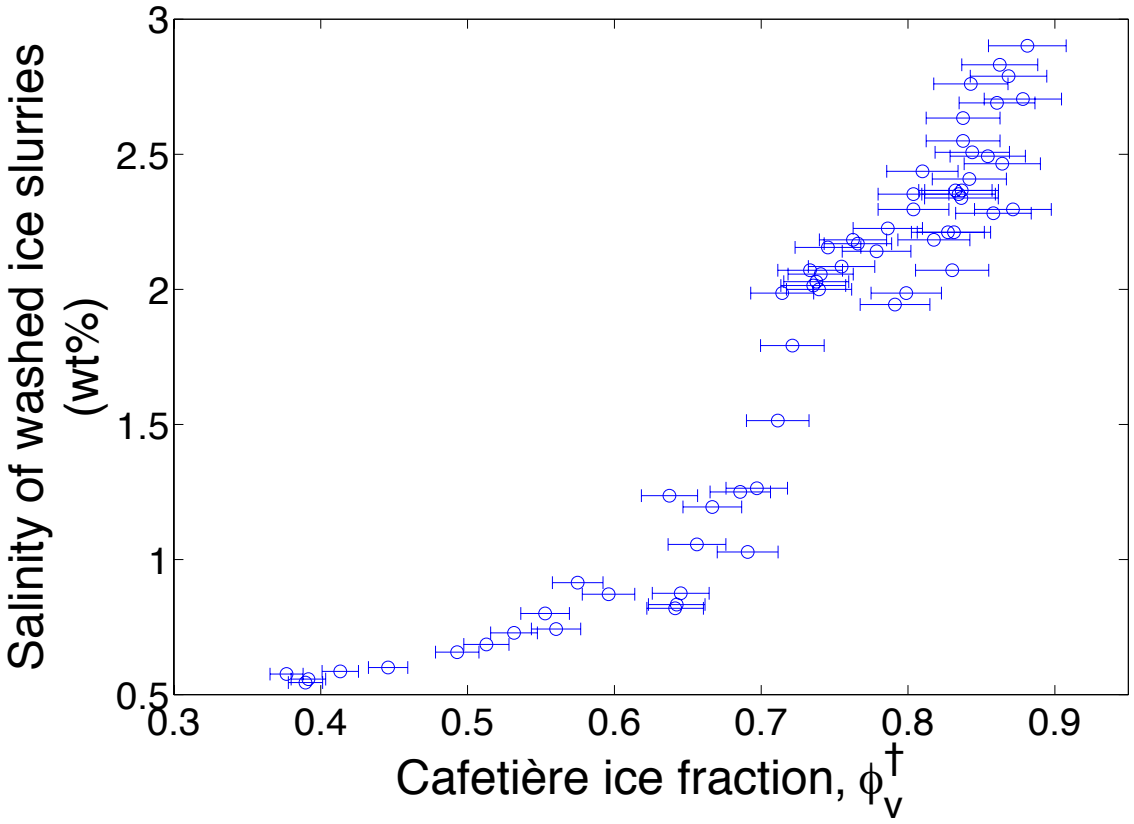

Figure 9: Slurry salinity vs. cafetière ice fraction

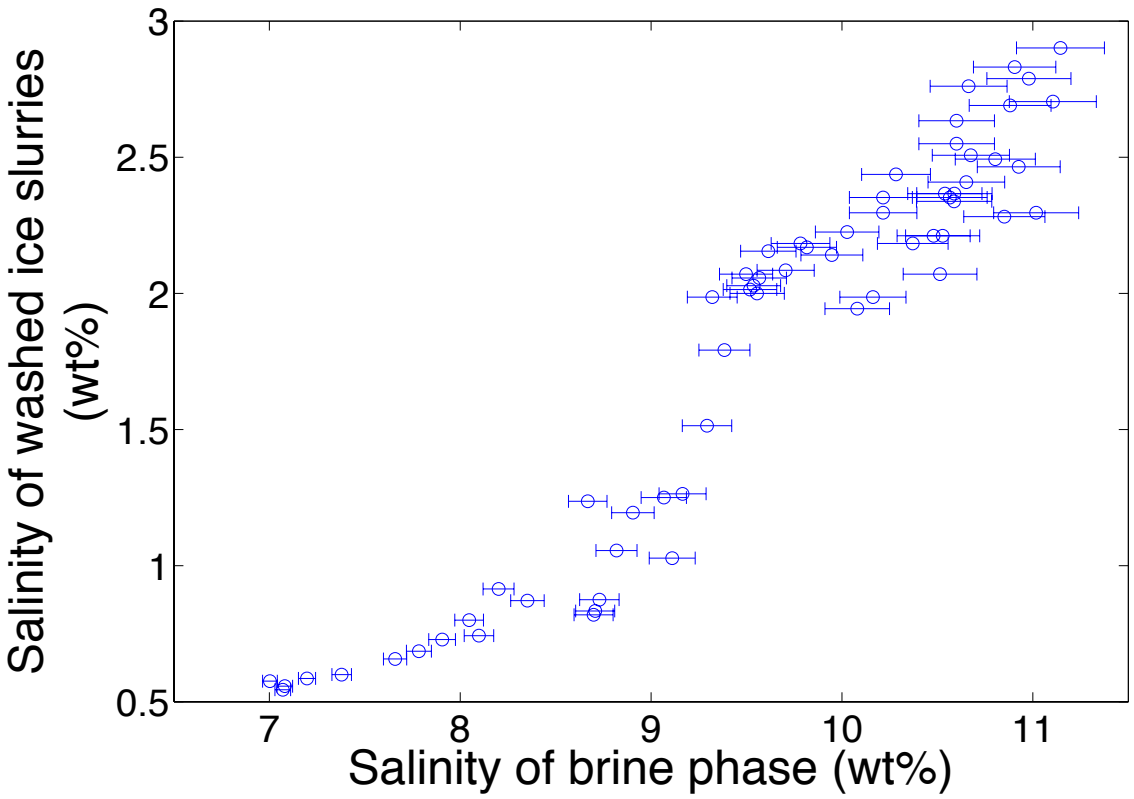

Figure 10: Slurry salinity vs. brine phase salinity

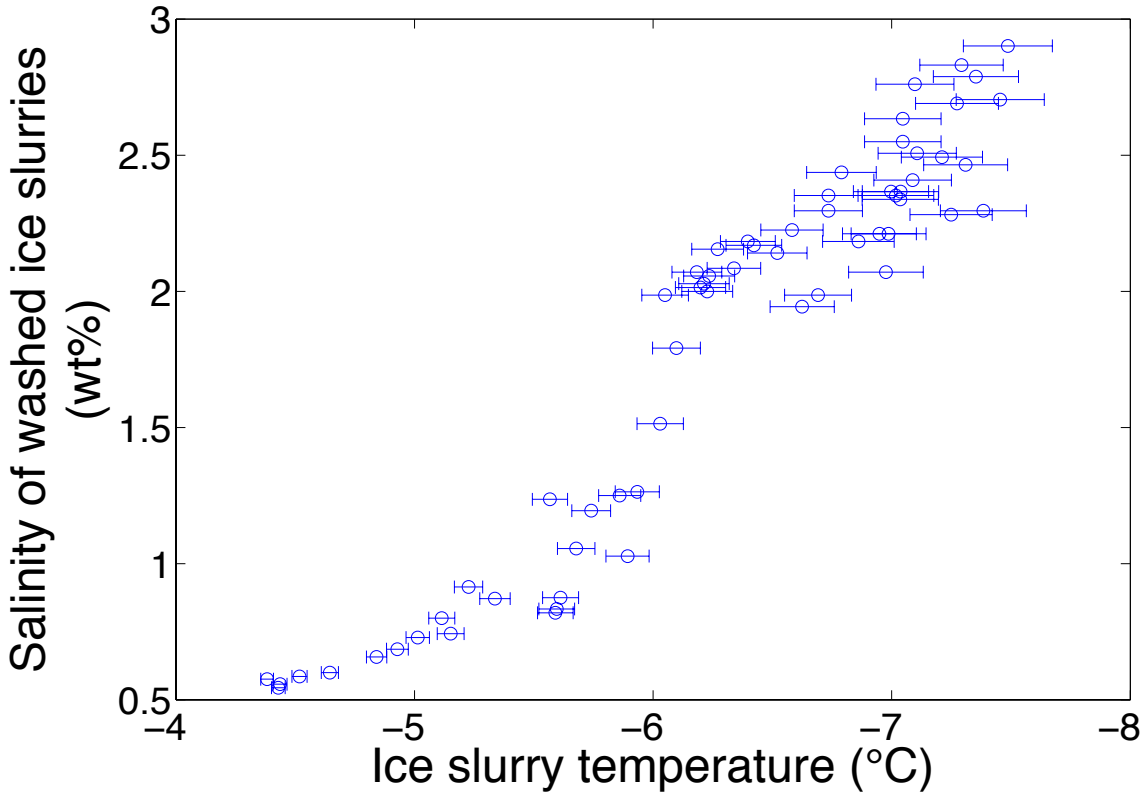

Figure 11: Slurry salinity vs. temperature

4.5 Effects of brine concentration

The change of the brine concentration alters the 'driving force' to mass transfer ($C_w - C_B$) and the conversion ratios are found improved by reducing the brine concentration from eutectic point. Figure 12 compares the conversion ratios of three brine concentrations (23.3%, 22% and 21%) and best fit lines are plotted with the data. The experiments were carried out at a range of bath temperatures. The conversion ratio drops linearly with the elevation of brine temperature in the cold bath in the form of $f(T_B) = p1 \times T_B + p2$ where $p1$ and $p2$ are coefficients. The values of these coefficients are listed in Table 1 for the studied brine concentrations.

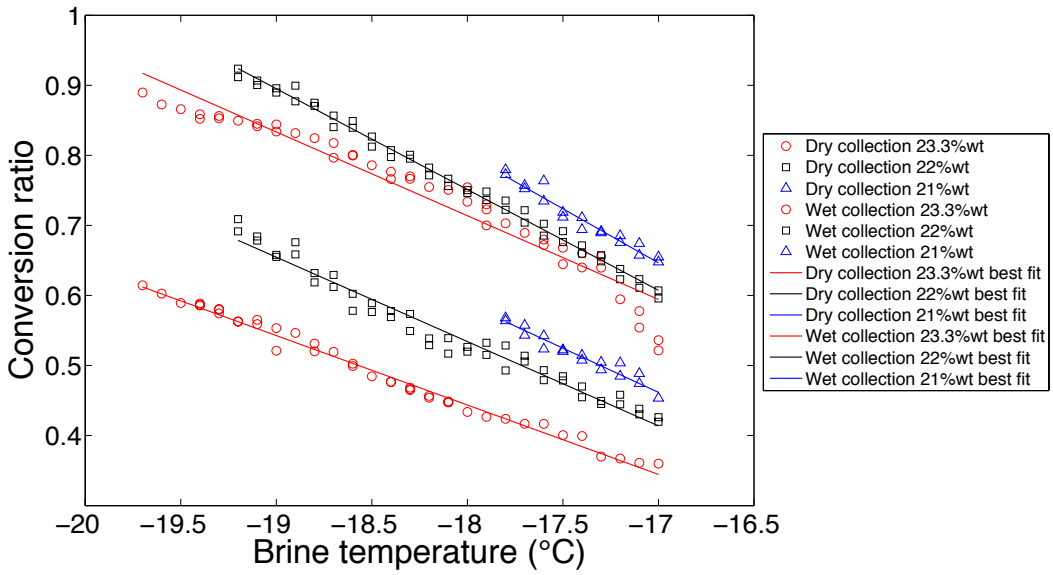

Figure 12: Conversion ratio comparison at different brine concentration with best fit line

Table 1: Coefficients of the best fit lines

	Dry collection		Wet collection	
Salt concentration (%wt)	$p1$	$p2$	$p1$	$p2$
23.3%	-0.09909	-1.34	-0.1196	-1.439
22%	-0.1204	-1.633	-0.1439	-1.839
21%	-0.1261	-1.682	-0.1545	-1.98

4.6 Freezing frontier

It is possible, by managing the flow rate and outlet angle, to have phase transformation to take place at a reasonably consistent distance from the tube outlet (Figure 13a and Video 2) and this steady state of ice generation can only be disturbed if the travelling ice reaches the brine surface. The location of the freezing frontier has evident impact on the morphology of the ice produced. Without phase transformation, the flow becomes more turbulent as it

travels further up in the cold environment and the generated ice, provided the ice can form, appears slushier than cases which water turns into ice while the flow is still at its laminar regime (Video 2). The morphology of ice generated in laminar and turbulent region are compared in Figure 13b and 13c.

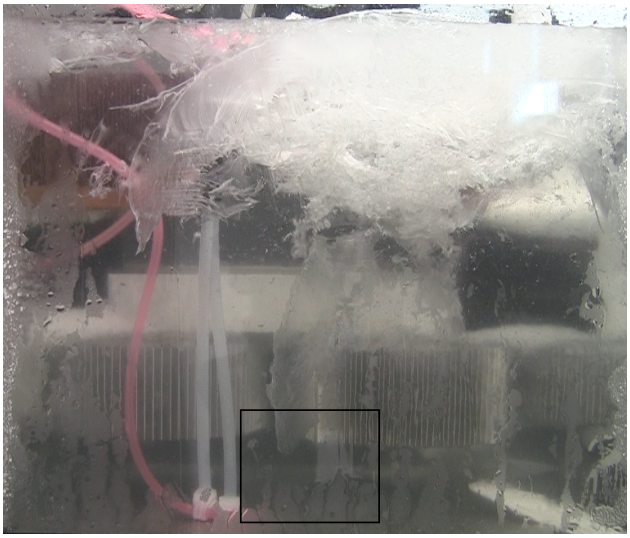

(a) Freezing frontier

(b) Sample ice formed in laminar region

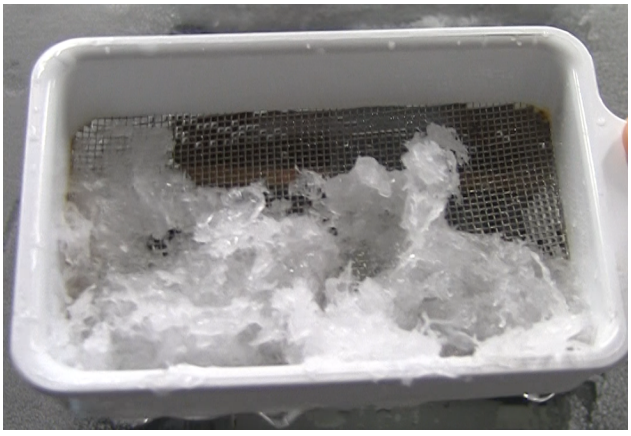

(c) Sample ice formed in turbulent region

Figure 13: Freezing frontier and collected ice sample

5 Optimisation of the cooling system

5.1 Evaporator temperature on COP

The craped surface ice makers require evaporator temperature, T_E, to operate at the range of -30 to -40℃ to achieve high rate of ice production. With low evaporator temperature, the surface area of the evaporator can be much smaller and hence reduce the size of and weight of the ice machine. The size of the ice maker is important for ice pigging because the equipments need to be shipped to the site of delivery. A low T_E, however, has unfavourable effect to the COP of the refrigeration system since more compressor work is required for a given duty. The COPs invariably worsen significantly as T_E drops, as shown in Figure 14. The blends, R404a and R57a that are refrigerants made of a number of refrigerants, exhibit slight lower COPs than the already banned and transitional refrigerants, but it is les significant compared to the change in T_E.

The assumptions made to calculate COPs of a cycle are:

- the compressor is in a healthy state, well lubricated and retains a constant isentropic efficiency, η_{isen}, of 70%
- pressure losses in suction and discharge line cause the temperature of the fluid to vary by 0.5 K
- useful subcooling and superheating are assumed to be 2 K
- condenser temperature, T_C, is assumed constant at 27℃
- unuseful superheat in the suction line, ΔT_{SLSH}, is 2 K

COP is defined by the ratio of available cooling by the refrigeration cycle, Q, and compressor work, W_c:

$$COP = \frac{Q}{W_c} \tag{6}$$

Q and W_c are determined by the relevant values of specific enthalpies for each temperature of the studied refrigerants.

In the experiments, the evaporator operates at -30℃ (Section 3.1) which is not much higher than most scraped surface ice makers, and this low temperature causes hydrohalite and ice to grow on the cold surface; the additional mass transfer generated by the pump is not sufficiently strong enough to stop phase transformation on the surface. Since the brine needs to be kept at a relatively quiescent state in order to reduce the chance of turbulence in the injected water stream, it is impractical to increase the power of the pump but to elevate the evaporator temperature to somewhere close to the eutectic point of brine and use some extended area of contact to achieve heat transfer needs.

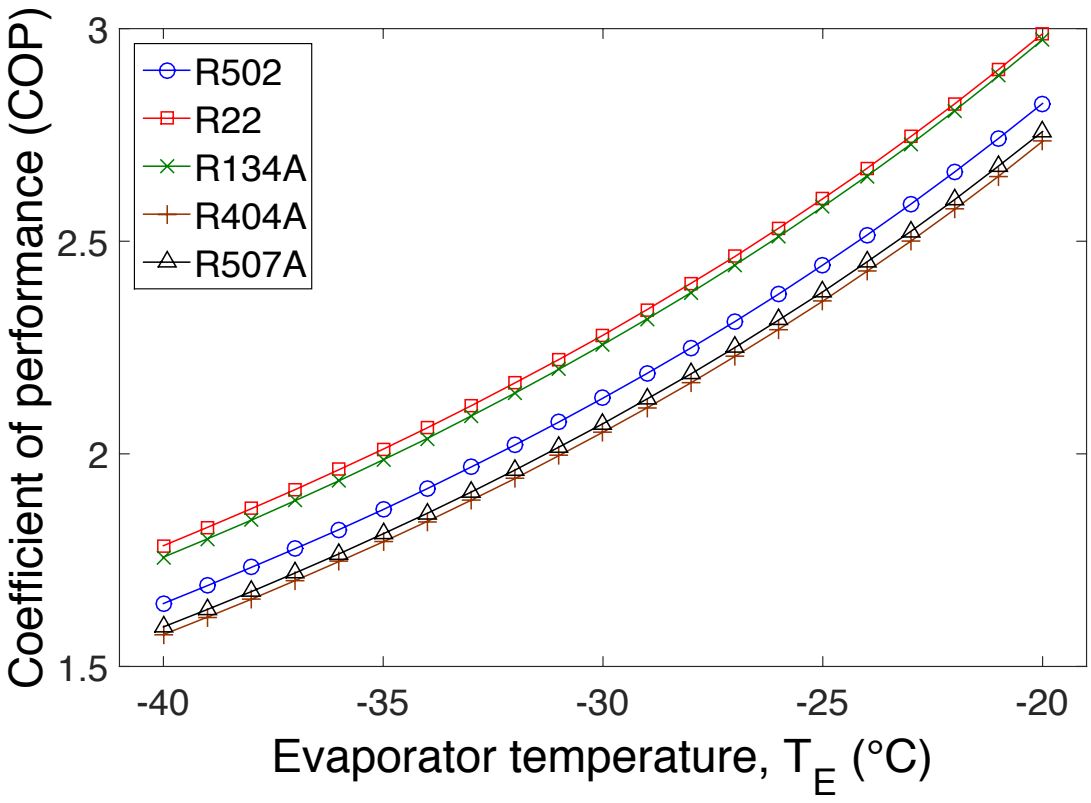

Figure 14: Coefficient of performance over a range of evaporator temperature

5.2 Evaporator and suctionline modification

The assumed 2 K unuseful superheat in the suctionline, as illustrated in Figure 15, causes the COPs to drop by roughly 1%. The model also suggests that for each 1 K of additional superheat in the suctionline, there is roughly a 0.5% decrease in COP. The amount of heat ingress into the refrigerant from the suctionline depends on the design of the system, insulation and ambient environment.

Water needs to be cooled down to a temperature close enough to its freezing point. Since the refrigerant is still very cold in the suction outlet, it is therefore possible to cascade a secondary heat exchanger between the evaporator outlet and suction inlet to extract the sensible heat from water instead of building another cooling system. In Figure 16, the model shows that COPs can be further increased by another 5 to 9% provided that the condenser inlet temperature is elevated to 10℃ by the additional cooling duty. In addition, the reduction of pressure ratio between suction and discharge absolute favours volumetric efficiency, η_{vol}, and hence the compressor efficiency.

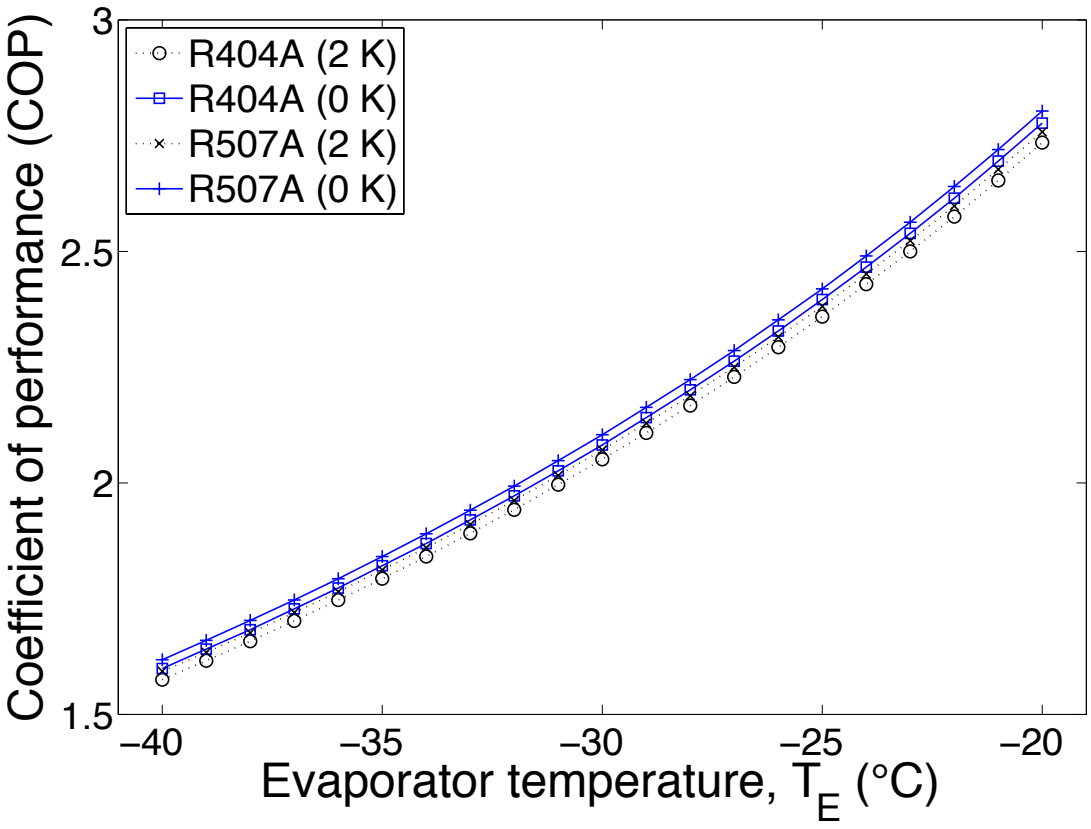

Figure 15: Effects of heat ingress into the suctionline (2 K and 0 K superheat)

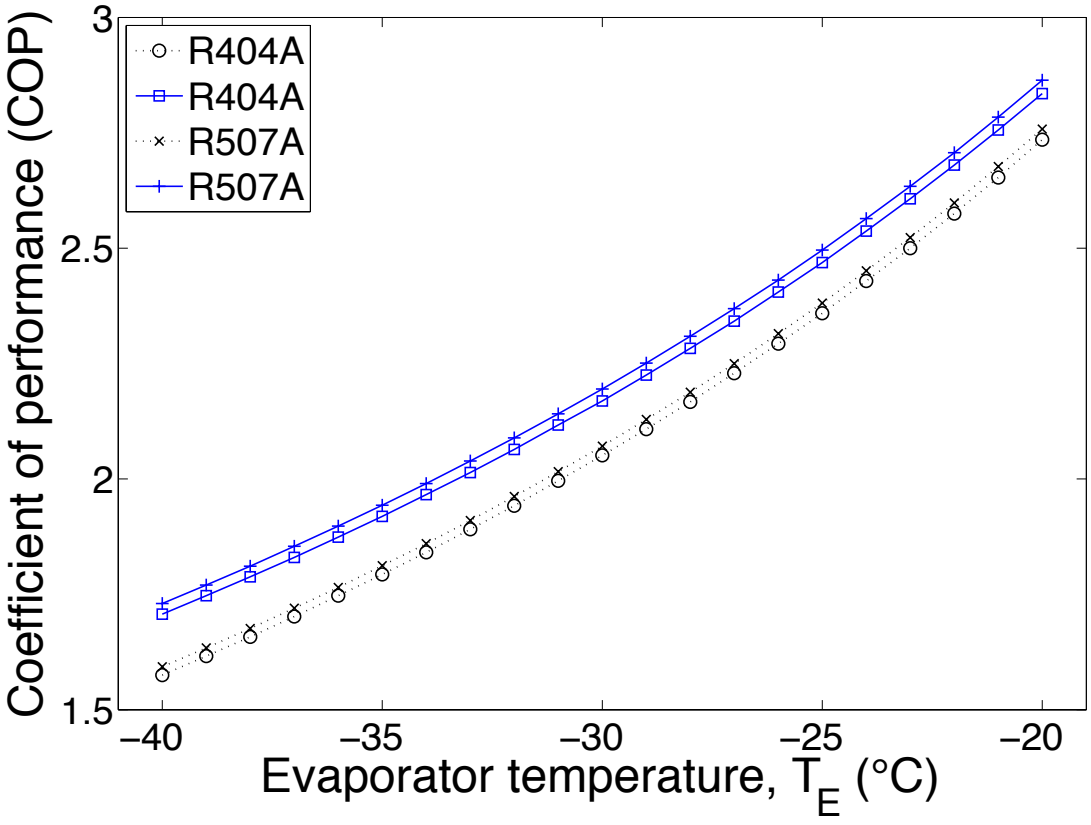

Figure 16: Effects of modified evaporator and suctionline

6 Conclusions

In practice, the concept of ice generation through introducing water into cold brine method works. The buoyancy force discourages mass transfer and therefore mixing if water is injected above the brine surface. Rate of growth reduces, as the ice grows thicker due to its low thermal conductivity. For the case that water is injected in the brine, flow rheology and area over volume ratio are important factors influencing ice growth. Flow with low level of turbulence and higher area over volume ratio assists ice generation.

The water to ice conversion ratio is sensitive to brine temperature and it is almost impossible to generate ice when brine temperature is -13℃ or higher. The conversion ratio changes linearly with the brine temperature. By washing the collected ice, the amount of salt in the ice drops from 13% to 1% and the mass of the ice collected would rise by 16 - 27% in the studied temperature range in comparison with the dry collection method. It was believed that the combination of the negative thermal inertia of the ice and water entrapment due to ice collapsing onto each other are the major reasons causing the difference in conversion ratio.

Reducing brine concentration in the cold bath can improve the water to ice conversion ratio under the studied salinity range. It is preferred to freeze water in its laminar region before it has turned turbulent because otherwise the level of mixing would rise and ice may not form. The position of freezing frontier has significant effects on morphology of the generated ice. Slushier ice is produced if the injected stream travels further up in the brine.

This way of ice production permits much higher evaporator temperature than the scraped surface method which means better COPs of the refrigeration system.

References

[1] C. Chaichana, W. W. Charters, and L. Aye, "An ice thermal storage computer model," *Applied Thermal Engineering*, vol. 21, no. 17, pp. 1769 – 1778, 2001.

[2] K. Matsumoto, M. Okada, T. Kawagoe, and C. Kang, "Ice storage system with water–oil mixture: formation of suspension with high {IPF}," *International Journal of Refrigeration*, vol. 23, no. 5, pp. 336 – 344, 2000.

[3] M. J. Wang and N. Kusumoto, "Ice slurry based thermal storage in multifunctional buildings," *Heat and Mass Transfer*, vol. 37, no. 6, pp. 597–604, 2001.

[4] J. Quarini, "Ice-pigging to reduce and remove fouling and to achieve clean-in-place," *Applied Thermal Engineering*, vol. 22, no. 7, pp. 747 – 753, 2002.

[5] A. J. Hales, G. Quarini, D. Ash, E. Lucas, and D. McBryde, "The use of ice pigging technology to clean shell and tube exchangers," *13th UK Heat Transfer Conference, UKHTC2013*, 2013.

[6] M. B. Lakhdar, R. Cerecero, G. Alvarez, J. Guilpart, D. Flick, and A. Lallemand, "Heat transfer with freezing in a scraped surface heat exchanger," *Applied Thermal Engineering*, vol. 25, no. 1, pp. 45 – 60, 2005.

[7] F. G. F. Qin, X. D. Chen, and A. B. Russell, "Heat transfer at the subcooled-scraped surface with/without phase change," *AIChE Journal*, vol. 49, no. 8, pp. 1947–1955, 2003.

[8] J.-P. Bedecarrats, T. David, and J. Castaing-Lasvignottes, "Ice slurry production using supercooling phenomenon," *International Journal of Refrigeration*, vol. 33, no. 1, pp. 196 – 204, 2010.

[9] B. Kim, H. Shin, Y. Lee, and J. Jurng, "Study on ice slurry production by water spray," *International Journal of Refrigeration*, vol. 24, no. 2, pp. 176 – 184, 2001.

[10] M. Hawlader and M. Wahed, "Analyses of ice slurry formation using direct contact heat transfer," *Applied Energy*, vol. 86, no. 7–8, pp. 1170 – 1178, 2009.

[11] N. Wijeysundera, M. Hawlader, C. W. B. Andy, and M. Hossain, "Ice-slurry production using direct contact heat transfer," *International Journal of Refrigeration*, vol. 27, no. 5, pp. 511 – 519, 2004.

[12] T. Kiatsiriroat, K. N. Thalang, and S. Dabbhasuta, "Ice formation around a jet stream of refrigerant," *Energy Conversion and Management*, vol. 41, no. 3, pp. 213 – 221, 2000.

[13] T. Kiatsiriroat, S. Vithayasai, N. Vorayos, A. Nuntaphan, and N. Vorayos, "Heat transfer prediction for a direct contact ice thermal energy storage," *Energy Conversion and Management*, vol. 44, no. 4, pp. 497 – 508, 2003.

[14] S. Thongwik, N. Vorayos, T. Kiatsiriroat, and A. Nuntaphan, "Thermal analysis of slurry ice production system using direct contact heat transfer of carbon dioxide and water mixture," *International Communications in Heat and Mass Transfer*, vol. 35, no. 6, pp. 756 – 761, 2008.

[15] A. Bejan, J. V. Vargas, and J. S. Lim, "When to defrost a refrigerator, and when to remove the scale from the heat exchanger of a power plant," *International Journal of Heat and Mass Transfer*, vol. 37, no. 3, pp. 523 – 532, 1994.

[16] V. Radcenco, J. V. C. Vargas, A. Bejan, and J. S. Lim, "Two design aspects of defrosting refrigerators," *International Journal of Refrigeration*, vol. 18, pp. 76 – 86, 2 1995.

[17] J. Vargas and A. Bejan, "Fundamentals of ice making by convection cooling followed by contact melting," *International Journal of Heat and Mass Transfer*, vol. 38, no. 15, pp. 2833 – 2841, 1995.

[18] A. Leiper, D. Ash, D. McBryde, and G. Quarini, "Improving the thermal efficiency of ice slurry production through comminution," *International Journal of Refrigeration*, vol. 35, no. 7, pp. 1931 – 1939, 2012.

[19] A. Leiper, *Carnot cycle optimisation of ice slurry production through comminution of bulk ice*. Phd thesis, Department of Mechanical Engineering, University of Bristol, 2012.

[20] A. Leiper, E. Hammond, D. Ash, D. McBryde, and G. Quarini, "Energy conservation in ice slurry applications," *Applied Thermal Engineering*, vol. 51, no. 1–2, pp. 1255 – 1262, 2013.

[21] G. S. F. Shire, *The behaviour of ice pigging slurries*. Phd thesis, Department of Mechanical Engineering, University of Bristol, 2006.

[22] T. S. Evans, *Technical Aspects of Pipeline Pigging with Flowing Ice Slurries*. Phd thesis, Department of Mechanical Engineering, University of Bristol, 2007.

[23] A. Hales, G. Quarini, G. Hilton, D. Ash, E. Lucas, D. McBryde, and X. Yun, "Ice fraction measurement of ice slurries through electromagnetic attenuation," *International Journal of Refrigeration*, vol. 47, pp. 98 – 104, 2014.

[24] H. J. Merk and J. A. Prins, "Thermal convection in laminary boundary layers. i," *Applied Scientific Research, Section A*, vol. 4, no. 1, pp. 11–24, 1953.

[25] H. J. Merk and J. A. Prins, "Thermal convection in laminar boundary layers ii," *Applied Scientific Research, Section A*, vol. 4, no. 3, pp. 195–206, 1954.

[26] H. J. Merk and J. A. Prins, "Thermal convection in laminar boundary layers iii," *Applied Scientific Research, Section A*, vol. 4, no. 3, pp. 207–221, 1954.

[27] J. H. Lienhard(IV) and J. H. Lienhard(V), *A Heat Transfer Textbook*. PHILOGISTON PRESS, 2008.

[28] A. Bejan, *Convection Heat Transfer, 4th Edition*. WILEY, 2013.

[29] N. H. Fletcher, *The Chemical Physics of Ice*. Cambridge U.P., 1970.

[30] C. S. Lindenmeyer and B. Chalmers, "Growth rate of ice dendrites in aqueous solutions," *The Journal of Chemical Physics*, vol. 45, no. 8, pp. 2807–2808, 1966.

[31] C. S. Lindenmeyer, G. T. Orrok1, K. A. Jackson, and B. Chalmers, "Rate of growth of ice crystals in supercooled water," *The Journal of Chemical Physics*, vol. 27, no. 3, pp. 822–822, 1957.

[32] H. R. Pruppacher, "Some relations between the structure of the ice-solution interface and the free growth rate of ice crystals in supercooled aqueous solutions," *Journal of Colloid and Interface Science*, vol. 25, no. 2, pp. 285–294, 1967.

[33] A. Bejan, S. Lorente, B. S. Yilbas, and A. Z. Sahin, "Why solidification has an s-shaped history," *Scientific Reports*, vol. 3, pp. 1711 EP –, 04 2013.

[34] A. Bejan and S. Lorente, "Constructal theory of generation of configuration in nature and engineering," *Journal of Applied Physics*, vol. 100, no. 4, 2006.

[35] D. R. Lide, *CRC Handbook of Chemistry and Physics*. Boca Raton: CRC Press, 86 ed., 2005.